<Title Page>

Article Type: Full Length Manuscript (FLM)

Title: Metal-induced streak artifact reduction using iterative reconstruction algorithms in X-ray CT image of the dento-alveolar region

Authors: Jian Dong, M. Eng.[*1], Yoshihiko Hayakawa, M.Sc., PhD[*1], Sven Kannenberg, B.Sc.[*2] and Cornelia Kober, Ph.D.[*2]

Institutional affiliation:

[*1] Dept. of Computer Science, Faculty of Engineering, Kitami Institute of Technology

[*2] Faculty of Life Sciences, Hamburg University of Applied Sciences, Hamburg, Germany

The corresponding author's address, phone, FAX, email account:

Jian Dong, Mr. (c/o Yoshihiko Hayakawa)

Dept. of Computer Science, Faculty of Engineering, Kitami Institute of Technology

165, Koen-cho, Kitami, Hokkaido 090-8507 JAPAN

Phone:+81-157-26-9326 (my lab.) FAX:+81-157-26-9344 (dept. office)

Email account: dongjian2007happy@yahoo.co.jp

Email account: d1171508045@std.kitami-it.ac.jp

Word count: abstract 150 words, manuscript 4202 words, 11 Figures and 2 Tables.

Disclosures:

Our joint research project was partly supported by the Bilateral Program of the Japan Society for the Promotion of Science, 2010-2012.

Abstract

Objective: To reduce metal-induced streak artifact on oral and maxillofacial X-ray CT (computed tomography) images by developing the fast statistical image reconstruction system using iterative reconstruction algorithms.

Study design: Adjacent CT images often depict similar anatomical structures in thin slices. So firstly images were reconstructed using the same projection data of an artifact-free image. Secondly images were processed by the successive iterative restoration method where projection data was generated from reconstructed image in sequence. Besides the maximum likelihood-expectation maximization algorithm, the ordered subset-expectation maximization algorithm (OS-EM) was examined. Also small ROI setting and reverse processing were applied for improving performance.

Results: Both algorithms reduced artifacts instead of slightly decreasing gray levels. The OS-EM and small ROI reduced the processing duration without apparent detriments. Sequential and reverse processing didn't show apparent effects.

Conclusions: Two alternatives in iterative reconstruction methods were effective for artifacts reduction. The OS-EM algorithm and small ROI setting improved the performance.

Clinical Relevance: (no more than 40 words)

We provide the clinically-applicable image processing technique to reduce metal-induced streak artifacts appeared on X-ray CT images and improve the visibility of anatomical structures in the oral and maxillofacial regions. Some modifications for improving the performance are examined.

INTRODUCTION

Since X-ray computed tomography (CT) imaging has some advantages in features of tissue and spatial resolutions, the bony and soft-tissue structures and related abnormalities are well-recognized for diagnosis. When X-ray computed tomography (CT) examinations are carried out in dental and maxillofacial regions and there are metallic prosthetic appliances in the oral cavity, the appearance of metal-induced streak artifacts is not avoidable.[1-8] Such artifacts are observed not only on multi-detectors row CT (MDCT) images but also on cone-beam CT (CBCT) images.[7,8] The fixed metallic prosthetic appliances are often made of high atomic-numbers and high-density materials. The streak artifacts are also caused by such dental fillings. Similar artifacts are also observed by the presence of other metallic biomaterials.[9-16]

Metallic biomaterials which are not only in the oral and maxillofacial region but also in other body regions cause the lack of the projection data due to high X-ray absorption coefficients.[4-6,10-12] The resulting sinogram patterns show the corruption by such missing data. It is known that the traditional CT reconstruction method, filtered back-projection (FBP) algorithm, cannot deal with such metal-induced inconsistencies. Some kinds of algorithms, however, have been proposed for the metal-induced streak artifact reduction.[4-6,9-16] They usually ~~took~~ take methods that the partly corrupted sinogram data are repaired by either the replacement of intact data or the relevant interpolation.

The analytic reconstruction algorithm, such as ~~the~~ FBP, is the gold standard on almost all modern CT systems in clinics.[4,17,18] On the contrary, statistical reconstruction algorithms are old idea but new technology for the quality improvement of CT images.[4,17-25] This has been applied for not only the image-quality improvement but also streak artifact reduction.[20,24,25]

In our previous studies, we focused on the fact that there were artifact-free slices in neighbor of slices having heavy streak artifacts but they depicted very similar anatomical structures. We

attempted on the maximum likelihood-expectation maximization (ML-EM) reconstruction algorithm and the successive iterative restoration to reduce metal-induced streak artifacts.[24,25] Kondo et al.[24] carried out the ML-EM algorithm to process a CT slice with heavy artifacts by using the projection data of the artifact-free slice on neighbor. There were seven slices (0.5 mm for a single slice) between the target slice and the artifact-free slice, namely they were apart for 3.5 mm in distance. The reduction of streak artifact was achieved, but some dimensional deviations were observed in the resultant images.[24] Then, Dong, et al. applied the successive iterative restoration method.[25] Firstly the projection data of the artifact-free slice was obtained. The adjacent slice, which showed weak artifacts, was processed. The projection data of the resultant image was used for the next neighboring slice. In this manner, the processing by the ML-EM and the computation of the projection data were repeated. The metal-induced streak artifact was well reduced on the resultant images and dimensional deviations were minimized. In general, statistical reconstruction algorithms necessitate the huge amount of computational efforts as they are sometimes called algebraic reconstruction technique. The ML-EM algorithm, which was employed in previous studies, was a time-consuming procedure.[24,25] It cost more than 6 mins to reconstruct a 512 x 512 matrix image for 50-cycle iterations using our desk-top PC.[25]

The ordered subset-expectation maximization (OS-EM) algorithm is the solution for the fast computation.[21,23] The OS-EM divides the projection data to several subsets and carries out the processing procedures for each subset in sequence, and the procedures are projection, back projection, comparison, and the data renewal which belong to the given subset. In this study, we developed the fast statistical image reconstruction system using the iterative reconstruction algorithm, OS-EM, for the reduction of metal-induced streak artifacts on the dento-alveolar CT images. Moreover, the effects of the small region of interest (ROI) setting, the successive processing and reverse processing methods were examined.

MATERIALS AND METHODS

Image acquisition

MDCT images of maxillary and partly mandibular jaws were acquired using a Somatom® Plus 4 Volume Zoom (Siemens, Erlangen, Germany). Principal exposure parameters were as follows: 120 kV, 130 effective mAs, and slice thickness was 0.5 mm. The pixel matrix of each slice was 512 x 512. The CT examination was carried out to examine as the pre-operative evaluation of the bone morphology in maxilla for the dental implant treatment. They were objects of the proposed processing procedures. The patient consented to the use of CT images for the study.

We acquired the original images in the order from head to foot. An artifact-free/intact slice was necessary for the iterative restoration method on the artifact reduction. Streak artifacts gradually appeared in many slices in maxilla and we could obtain an artifact-free CT slice which was immediate neighbor to the first CT slice with weak artifacts in the head direction. The successive processing, to be hereinafter described, started at the combination of these two neighboring CT slices.

First, we applied the successive method to twelve images in maxilla as shown in **Fig. 1.** They had weak or severe metal-induced streak artifacts. They occurred at either one or several tooth crowns and as a result overlapped regions were invisible. Also we applied the same method to eight images in mandible as shown in **Fig. 2.** Since this was a case of the CT examination for the pre-implant operation in maxilla, we could not find an artifact-free CT slice in mandible. Weak artifacts were still observed at the bottom right slice.

Projection data acquisition

Projection data acquisition was carried out as described in the previous paper.[24,25] Each pixel on the image has a CT number, which is proportional to the X-ray transparency. When the X-ray projection traverses each pixel, the shape of each pixel is usually a trapezoid depending on the angle between

the projection and each pixel square. In special cases, projection shapes of square pixels become either a square at 0°, 90°, 180°, and 270° or a triangle at 45°, 135°, 225°, and 315° when the coordinate axes are set along edges of the image. There is a detector containing 512 pixels whose value is called detectability. During the detectability calculation, the value is accumulated by adding the respective pixels' CT number. If the shape of the projection is not square, the detectability ~~is~~ will be divided by the center of the detector element and neighboring elements. The projection data were acquired at 360 directions with 1° intervals, so the pixel number was 512 x 360. As an example, an artifact-free/intact image, which is the next image to the first one at the far-left side on the top row in **Fig. 1**, and the projection data (sinogram) computed from the artifact-free image are shown in **Fig.3 (A, B)**.

In this work, we chose two ways to process the images in maxillary CT images. In one way, we first got the projection data of the artifact-free image, namely the image which appeared in **Fig. 3A.** The continuous 12 images were all processed using the same intact image's projection data. In the other way, the projection data acquisition of the artifact-free image (**Fig. 3A**) was carried out similarly. We used this projection data to reduce the artifact of Image No.1, the far left one on the top row in **Fig. 1**. After Image No.1 was reconstructed, we got the projection data of the processed Image No.1, and applied it to process Image No.2 on neighbor. As so on, we used the successive iterative restoration method for processing 12 images in **Fig. 1**.

Iterative restoration: ML-EM and OS-EM methods

Generally CT examinations with thin slice thicknesses are carried out in the oral and maxillofacial regions. And adjacent images often depicted very similar anatomical structures. So our trial is to reconstruct the CT image containing streak artifacts using the projection data of the adjacent image. The processing starts at the CT slice having weak streak artifacts where there is an artifact-free slice

at the next. Secondly, the next image having still weak streak artifacts ~~was~~ will be processed using the projection data of the former artifact-reduced image. And the same process ~~was~~ will be applied to the next images.

The ML-EM algorithm is an iterative restoration method that results in an approximation between the processing image and the target image. The formulation of ML-EM algorithm is described as follows:

$$\lambda_j^{(k+1)} = \frac{\lambda_j^{(k)}}{\sum_{i=1}^{n} C_{ij}} \sum_{i=1}^{n} \frac{y_i C_{ij}}{\sum_{j'=1}^{m} C_{ij'} \lambda_{j'}^{(k)}}$$

The λ (Lambda) is the output value of each pixel. Other parameters are as follows;

k : the counter of iteration (loop variable)

j : the number of pixel (1-m), m = 262,144 if the image matrix is 512 x 512.

i : the number of detector's element (1-n)

C_{ij} : detectability as the relation of pixel (i) and detector's element (j)

y_i : the projection data by the pixel (i)

We applied the ML-EM algorithm to reconstruct images following the steps shown in **Table I**. In step 2, it is a process of comparing the projection data under processing to the intact image's projection data. And then make an approximation between them which is a key step. We set the parameter of iteration times as 50, because in our previous report we have proved that the reduction effect was almost the same when the iteration times were set either 50 or 100 times.[24,25]

The OS-EM algorithm was also employed as the successive iterative reconstruction algorithm in this work. The OS-EM algorithm which is based on the ML-EM algorithm divides the projection data to several subsets and carries out the projection, comparison, renewal, and back projection to just the data belonged to the given subset. Subsets of a 24 projection angles example are

schematically shown in **Fig.4.** The 24 projection angles can be divided into {1, 2, 3, 4, or 6} subsets as shown in **Fig.4.** For the OS-EM algorithm, the image quality factor, namely the image update number, is the product of subset numbers and iteration times (image update number = subset number x iteration times). Therefore, there will be more image updates during one time iteration and as a result images can be reconstructed quickly. In our previous report, combinations of subset number (either 4 or 8) and iteration numbers (either 5 or 10) were examined.[26] As the result, the optimal combination of subset number and iteration times was derived to be subset=8 and iteration=10, and streak artifacts could be reduced at utmost on this condition.[26] Then we chose this combination decisively in this study.

Successive iterative restoration

In our previous study, Kondo et al.[24] applied the ML-EM algorithm on a single CT slice with heavy streak artifacts. They examined effects of repeated times of the iteration, which were ranging from 1 to 100, and indicated that 50 iterations were enough to achieve the artifact reduction. Streak artifacts were reduced effectively but slight deviations in anatomical structures appeared surrounding teeth and soft tissues.

In our another previous study, Dong et al.[25] applied the successive iterative restoration. They showed twelve neighboring images which were processed in this way and observed the slight improvement in the anatomical structure reproducibility.[25] We call this method the successive iterative restoration and apply the method on this study.

First, we applied the successive method to twelve maxilla images as shown in **Fig. 1**. They had either weak or severe metal-induced streak artifacts. They occurred at either one or several tooth crowns and as a result overlapped regions were invisible. Then we also applied the successive iterative restoration to mandible region as shown in **Fig.2.**

Region of interest setting

Since streak artifacts only appeared surrounding the teeth, we did the segmentation to CT slices to restrict only the teeth region. A simple rectangular ROI (region of interest) was used for the segmentation. As an example, the segmented artifact-free slice and its projection data are shown in **Fig. 5 (A, B).** The pixel matrix of each segmented slice was 512 x 295. The projection data were calculated only from the teeth area, therefore the density of the center part became brighter in the projection data image (sinogram), and comparatively the soft tissues' components seemingly disappeared at the image peripherals.

Reverse processing

As described in sections in advance, the successive processing was carried out mainly on maxillary region and CT slices were processed along the head-to-foot direction. We call this the forward processing. On the other hand, we tried the reverse processing in the mandible region as shown in **Fig. 2**. Namely, the successive processing carried out along the foot-to-head direction.

We did reverse processing to 7 mandible images as shown in **Fig. 2**. The bottom right one was used for a quasi-intact image. The successive iterative OS-EM algorithm was employed and the same above-mentioned optimal combination parameter setting was chosen. First, the projection data of Image No.8 (at the far-right on the bottom row) in **Fig. 2** was achieved, then applied the projection data to reconstruct Image No.7 in neighbor. The reconstructed Image No.7 was used to reconstruct Image No.6 and so on.

PC performance

The PC which we used had an Intel^{R} Core^{TM} 2 Duo CPU running at 3.16 and 2.83 GHz and Windows Vista OS.

RESULTS

The continuous 12 images showed in **Fig. 6** were reconstructed by the ML-EM algorithm using the same projection data of the intact image. These maxillary images are corresponding to twelve images in **Fig. 1**. Streak artifacts were reduced. The high density parts were reduced. However, some artifacts still remained on the resultant images.

Figure 7 shows 12 resultant images processed by ML-EM successive iterative algorithm. These maxillary images are corresponding to twelve images in **Fig. 1**. The projection data they used were generative ones. Namely image No.2 was processed using the projection data of reconstructed image No.1, and image No.3 was processed using reconstructed image No.2 and so on. Artifacts on them seemed to be reduced as similar as those in **Fig. 6**. The second molar tooth on the left mandible was overlapped absolutely with artifacts in the original image, however, after the processing it became clear to some extent.

Twelve reconstructed images processed by the OS-EM successive iterative algorithm are shown in **Fig. 8**. The initially inputted projection data was the same as that of ML-EM successive iterative processing. We set subset number (8) and iteration times (10), so each image was updated for 80 times. The artifact reduction effect was observed as similar as those in Fig. 6 and Fig. 7. The high density parts were reduced.

We show the zooming pictures for easy observing as **Fig.9**. The two images in the first column were taken from **Fig.1**. They are zooming pictures from molar and mandibular ramus regions in No.4 and No.8 images of **Fig.1**. And as so on, the two images in the second column were taken from **Fig.6**. They are zooming pictures from molar and mandibular ramus regions in No.4 and No.8 images of **Fig.6**. The images in the third and forth column were taken from the same parts of **Fig.7** and **Fig.8** respectively.

The segmented ROI images were also processed by the OS-EM successive iterative algorithm in

the condition of the optimal parameter combination, and the results are shown in **Fig.10**.The teeth region was reconstructed without the influence of posterior tissues, and streak artifacts were reduced.

Four subtracted images are shown in **Fig.11**. They are subtracted images between the original image No.4 of Fig.1 and corresponding No.4 resultant images of respective methods. (Image No.4 of **Fig. 6**, **Fig. 7**, **Fig. 8** and **Fig.10** from left to right). The subtracted images contained streak artifacts reduced by mentioned algorithms. Anatomical structures were also recognized to some extent, so it demonstrated that the dimensional reproducibility was affected on the reconstructed images.

We did reverse processing to 7 mandible images, namely the successive processing, was carried out along the foot-to-head direction. The reconstructed images by the successive iterative OS-EM algorithm are shown in **Fig.12**. Since there existed a little streak artifacts although on the assumed intact image (No. 8) of mandible slices, streak artifacts weren't reduced exhaustively.

Processing time is an important factor for clinical operation. **Table II** shows the duration time ratio of each method. It cost 6 min 10 sec for processing a slice by the ML-EM algorithm and we regarded the time as 1 unit. It demonstrated that the OS-EM algorithm is a time saving method. And the ROI segmentation processing can further short the processing time to about one eighth of the ML-EM method.

For the result images, the output image density became lower as the CT number increased. To get rid of the influence to artifact reduction by the lower density, we did approximate contrast enhancement to each result image.

DISCUSSION

In our previous studies the ML-EM algorithm was proved to be effective for reducing streak artifacts on X-ray CT images.[24,25] As the successive iterative reconstruction algorithm, both ML-EM and OS-EM algorithms were employed in this study. Algorithms practically performed a process of

the successive correction to individual slice. We chose the successive iterative method because adjacent CT slices often depict very similar anatomical structures among thin-thickness slices. However, differences were not obviously observed between Fig. 6 and Figs. 7 &8.

The OS-EM algorithm divides the projection data to several subsets, but when subset number equals one, the process is the same with that of ML-EM algorithm. For the OS-EM method, image update number (= subset number x iteration times) was set. The parameter setting procedure was described in our previous report.[26] We chose one of them, but differences in the quality of resultant images was not large, therefore we do not present all resultant images to avoid the redundant description. Then there will be more image updates in one iteration than the ML-EM method, and streak artifacts could be reduced for a small number of iterations by the OS-EM algorithm. In our previous report, the successive method in the iterative restoration had a merit in the reproducibility of anatomical structures.[25] Especially differences in the high-contrast dental enamel area was thought to be emphasized. We applied our processing methods to another clinical case in this study. It is thought that this case shows too severe metal-induced streak artifacts to express differences.

There are two advantages of ROI image segmentation. On one hand, during image reconstruction, influence from posterior tissues structure was removed. On the other hand, the processing time for reconstructing one image was shorten significantly, to about a half. The segmentation was done by cutting the top and bottom parts without teeth structure, and we are considering segmenting the image along the maxillary edge line in the next step.

The iterative restoration is an approximation process to the target image. It is important to select a target image. For the maxillary images, streak artifacts appeared gradually, so we can get the artifact-free image which serves as the target image. The projection data calculated from the artifact-free image was not influenced by artifacts and that's the key point for the successful reduction. On the contrary, in the reverse processing of the mandible images, there was not an image without

streak artifacts, so in the result images, some of streak artifacts never disappeared.

The time required for the calculation was not only dependent on the PC performance, but also dependent on the amount of streak artifacts[25]. The OS-EM algorithm is the method used to reduce the calculation time in comparison with the ML-EM algorithm. It is clinically used for PET and SPECT examinations in nuclear medicine.[25] The OS-EM algorithm is an efficient method for the streak artifact removal from CT images.

A contrast enhancement was carried out on each resultant image. It was the difficulty this time to control the overall density and contrast of the processed CT images in comparison with our previous reports on the ML-EM algorithm.[24,25] In particular, the overall density and contrast became dark and low at the processing of Image No. 9 to No. 12 on the bottom row in Fig. 1. We think that this is due to the existence of too severe metal-induced streak artifacts.

The processing procedures for the metal-induced streak artifact reduction have still not been fully-automatic. This is the requirement for the practical use. However, we described our concepts, modifications in methods, and the practical example here.

In conclusion, the streak artifact reduction in dental-alveolar CT images was achieved by the iterative restoration methods and the modified successive method. Both ML-EM and OS-EM algorithms were adopted. For the ML-EM algorithm, we set 50 cycles for each processing, and for OS-EM algorithm, we set subset number=8 and iteration times=10. Subtracted images were calculated as the reference of reduction effectiveness and the reproducibility of anatomical structures. Both algorithms reduced metal-induced artifacts on the contrary of slight decreasing of gray levels for severe-artifact images. The OS-EM algorithm and small ROI setting reduced the processing duration without apparent detriments. Successive and reverse processing methods did not show apparent effects.

REFERENCES

1. Miracle AC, Mukherji SK. Conebeam CT of the head and neck, part 2: clinical applications. Am J Neuroradiol 2009;30:1285–92.
2. Shimamoto H, Kakimoto N, Fujino K, Hamada S, ShimosegawaE, Murakami S, et al. Metallic artifacts caused by dental metal prostheses on PET images: a PET/CT phantom study using different PET/CT scanners. Ann Nucl Med 2009;23:443–9.
3. Nahmias C, Lemmens C, Faul D, Carlson E, Long M, Blodgett T, et al. Does reducing CT artifacts from dental implants influence the PET interpretation in PET/CT studies of oral cancer and head and neck cancer? J Nucl Med 2008;49:1047–52.
4. Boas FE, Fleischmann D. Evaluation of two iterative techniques for reducing metal artifacts in computed tomography. Radiology 2011;259: 894-902.
5. Tohnak S, Mehnert AJH, Mahoney M, Crozier S. Dental CT metal artifact reduction based on sequential substitution. Dentomaxillofac Radiol 2011;40:184-90.
6. Abdoli M, Ay MR, Ahmadian A, Dierckx RA, Zaidi H. Reduction of dental filling metallic artifacts in CT-based attenuation correction of PET data using weighted virtual sinograms optimized by a genetic algorithm. Med Phys 2010;37:6166-77.
7. Bechara BB, Moore WS, McMahan CA, Noujeim M. Metal artefact reduction with cone beam CT: an in vitro study. Dentomaxillofac Radiol. 2012;41:248-53.
8. Bechara B, McMahan CA, Geha H, Noujeim M. Evaluation of a cone beam CT artefact reduction algorithm. Dentomaxillofac Radiol. 2012;41: published ahead of print Feb. 23, 2012.
9. Liu PT, Pavlicek WP, Peter MB, Spangehl MJ, Roberts CC, Paden RG. Metal artifact reduction image reconstruction algorithm for CT of implanted metal orthopedic devices: a work in progress. Skeletal Radiol 2009;38:797-802.

10. Joemai RM, de Bruin PW, Veldkamp WJ, Geleijns J. Metal artifact reduction for CT: development, implementation, and clinical comparison of a generic and a scanner-specific technique. Med Phys 2012;39:1125-32.
11. Veldkamp WJ, Joemai RM, van der Molen AJ, Geleijns J. Development and validation of segmentation and interpolation techniques in sinograms for metal artifact suppression in CT. Med Phys 2010;37:620-8.
12. Zhang Y, Zhang L, Zhu XR, Lee AK, Chambers M, Dong L : Reducing metal artifacts in cone-beam CT images by preprocessing projection data. Int J Radiat Oncol Biol Phys 2007;67:924–32.
13. Prell D, Kyriakou Y, Beister M, Kalender WA. A novel forward projection-based metal artifact reduction method for flat-detector computed tomography. Phys Med Biol 2009;54:6575-91.
14. Rinkel J, Dillon WP, Funk T, Gould R, Prevrhal S. Computed tomographic metal artifact reduction for the detection and quantitation of small features near large metallic implants: a comparison of published methods. J Comput Assist Tomogr 2008;32:621–9.
15. Moon SG, Hong SH, Choi JY, Jun WS, Kang HG, Kim HS, et al. Metal artifact reduction by the alteration of technical factors in multidetector computed tomography: a 3-dimensional quantitative assessment. J Comput Assist Tomogr 2008;32:630–3.
16. Bal M, Spies L. Metal artifact reduction in CT using tissue-class modeling and adaptive prefiltering. Med Phys 2006;33:2852–9.
17. Fleischmann D, Boas FE. Computed tomography--old ideas and new technology. Eur Radiol 2011;21: 510-7.
18. Pan X, Sidky EY, Vannier M. Why do commercial CT scanners still employ traditional, filtered back-projection for image reconstruction? Inverse Probl. 2009;25:1230009.
19. Rashed EA, Kudo H. Statistical image reconstruction from limited projection data with intensity priors. Phys Med Biol. 2012;57:2039-61.

20. Wang G, Frei T, Vannier MW. Fast iterative algorithm for metal artifact reduction in X-ray CT. Acad Radiol 2000;7:607–14.
21. Gutman F, Gardin I, Delahaye N, Rakotonirina H, Hitzel A, Manrique A, et al. Optimisation of the OS-EM algorithm and comparison with FBP for image reconstruction on a dual-head camera: a phantom and a clinical 18F-FDG study. Eur J Nucl Med Mol Imaging 2003;30: 1510-9.
22. Hwang D, Zeng GL. Convergence study of an accelerated ML-EM algorithm using bigger step size. Phys Med Biol 2006;51:237–52.
23. Xu F, Xu W, Jones M, Keszthelyi B, Sedat J, Agard D, et al. On the efficiency of iterative ordered subset reconstruction algorithms for acceleration on GPUs. Comput Methods Programs Biomed 2010;98: 261-70.
24. Kondo A, Hayakawa Y, Dong J, Honda A. Iterative correction applied to streak artifact reduction in an X-ray computed tomography image of the dento-alveolar region. Oral Radiol 2010;26: 61–65.
25. Dong J, Kondo A, Abe K, Hayakawa Y. Successive iterative restoration applied to streak artifact reduction in X-ray CT image of dento-alveolar region. Int J Comput Assist Radiol Surg 2011; 6:635-40.
26. Dong J, Kondo A, Abe K, Hayakawa Y, Kannenberg S, Kober C. Metal artifact reduction by ordered subset-expectation maximization reconstruction algorithm on X-ray computed tomography image. A reviewed article in the Proceedings of Forum on Information Technology 2011, Sep. 2011, Hakodate, Japan. (http://www.ipsj.or.jp/10jigyo/fit/fit2011/, *in Japanese*)

FIGURE LEGENDS (CAPTIONS)

Fig.1 Continuous twelve images are aligned from Head to Foot, from No.1, the far left side on the top row, to No. 12, the far right side on bottom row. They are original maxillary images on which streak artifacts appeared and objects for the proposed processing.

Fig.2 Continuous eight lower jaw images aligned from Head to Foot. The artifact-free image didn't exist because the range of exposures.

Fig. 3(A, B) A**:** The artifact-free/intact image, which is next to Image No. 1 of Fig. 1.

B**:** The projection data computed from the artifact-free image of Fig.3 A.

Fig.4 The OS-EM subsets combination. There are 24 projection directions in this example.

Fig. 5(A, B) A**:** The segmented artifact-free/intact image, whose original image is next to Image No.1 of Fig. 1.

B**:** The projection data computed from Fig.5 B.

Fig.6 The reconstructed 12 images by ML-EM algorithm using the same artifact-free image's projection data. They are corresponding to the order of Fig.1.

Fig.7 Reconstructed images of Image No.1 to No. 12 by successive iterative ML-EM algorithm. They are corresponding to the twelve images in Fig 1.

Fig.8 Reconstructed images of Image No.1 to No. 12 by successive iterative OS-EM algorithm, They are corresponding to the twelve images in Fig 1.

Fig.9 Zooming pictures. The two images in the first column were taken from Fig.1. They are zooming pictures from molar and mandibular ramus regions in No.4 and No.8 images of Fig.1. And as so on, the two images in the second column were taken from Fig.6. They are zooming pictures from molar and mandibular ramus regions in No.4 and No.8 images of Fig.6. The images in the third and forth column were taken from the same parts of Fig.7 and Fig.8 respectively.

Fig.10 Reconstructed ROI images of Image No.1 to No. 12 by successive iterative OS-EM algorithm. They are corresponding to the twelve images in Fig 1.

Fig.11 Four subtracted images between original image No.4 (No.4 image of Fig.1) and corresponding No.4 result images of respective method (No.4 image of Fig.6, Fig.7, Fig.8 and Fig.10).

Fig.12 Reconstructed lower jaw images of No.1 to No. 7 by successive iterative OS-EM algorithm.

FIGURES and TABLES

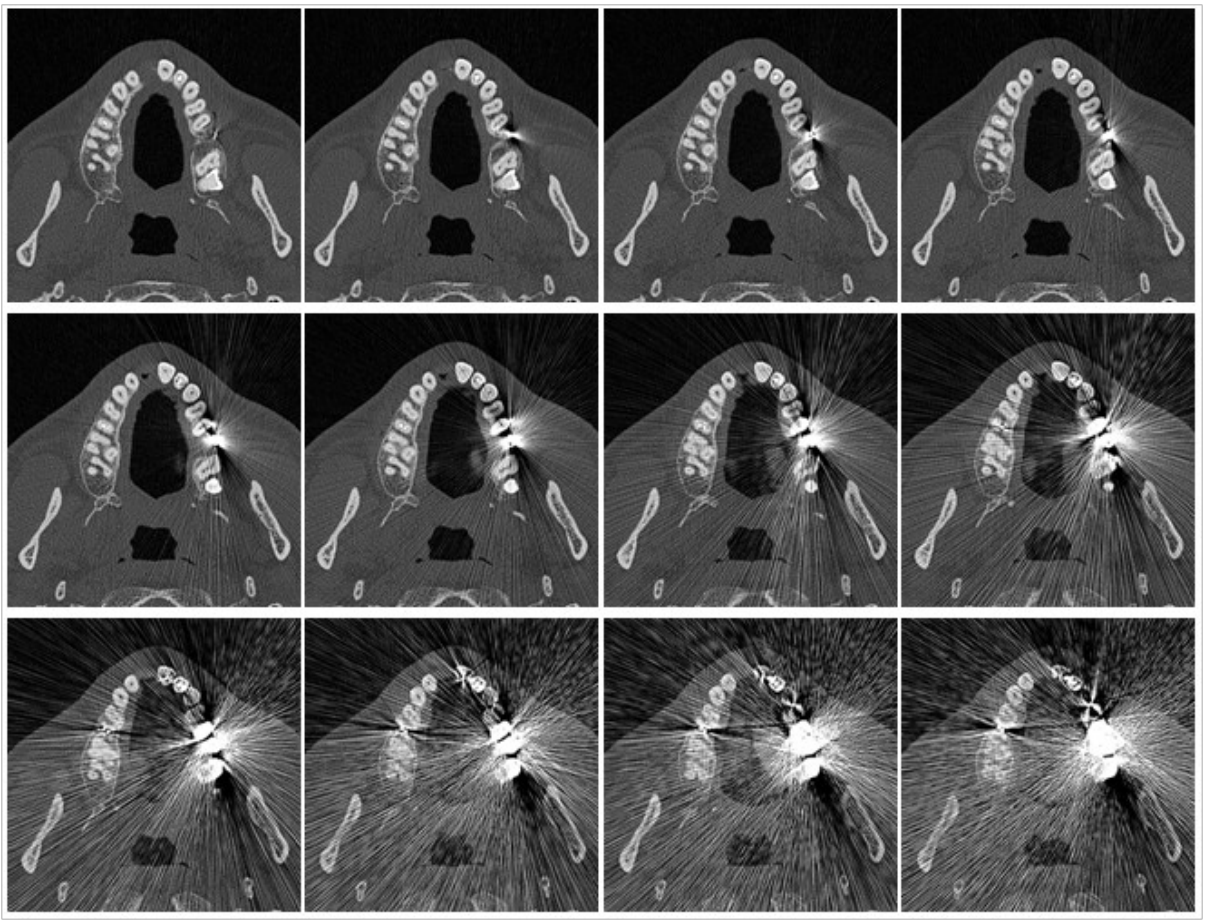

Fig.1

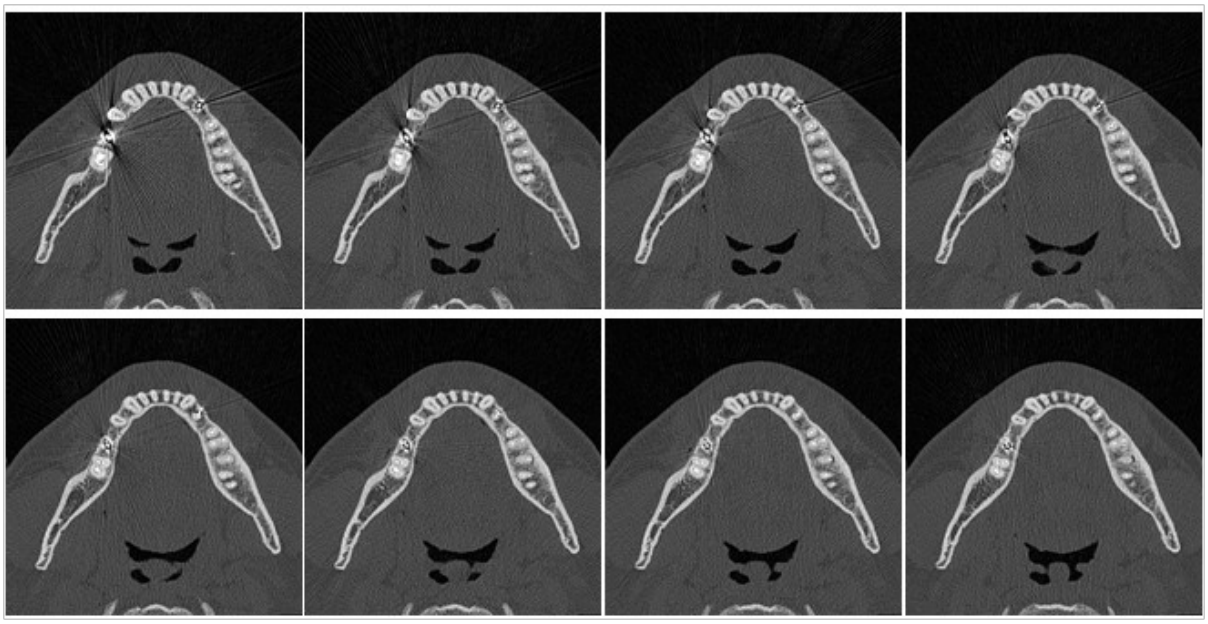

Fig.2

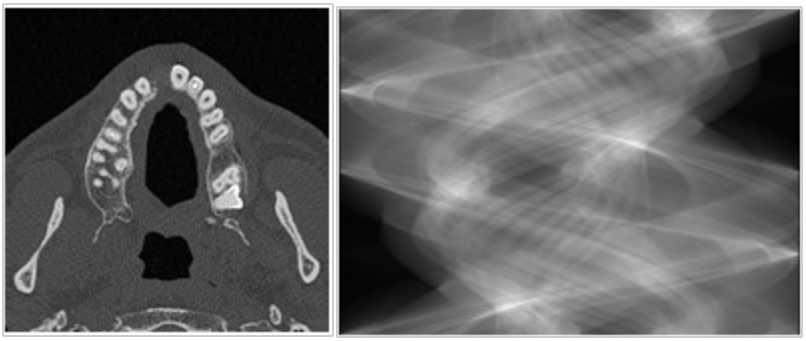

Fig. 3(A, B) A**:** B**:**

Table I. The flow of the ML-EM algorithm

Step	Procedure
Step 1	Select Image No.1 and get its projection data
Step 2	Compare the projection data of the intact image with that of Image No.1 and do the correction to Image No.1's projection data
Step 3	Compute the correction coefficient
Step 4	Reconstruct Image No.1 by back projection of the renewed projection data
Step 5	Repeat from Step 2 to Step 4
Step 6	Stop iteration when it meets the end condition and get processed image

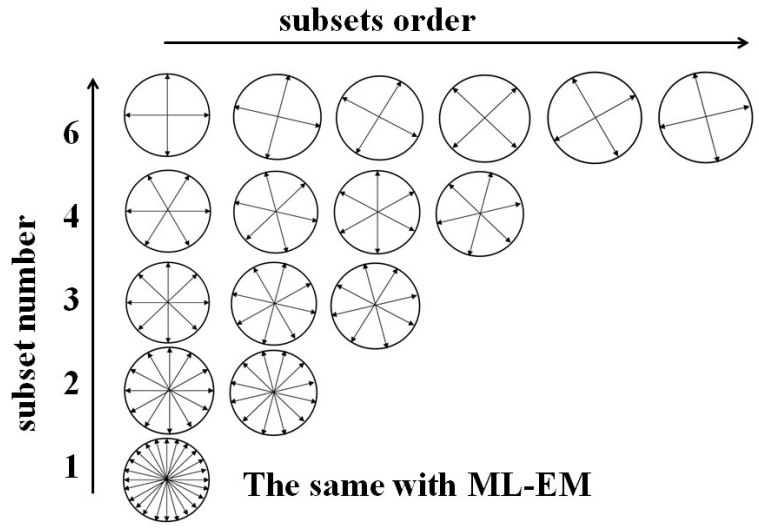

Fig.4

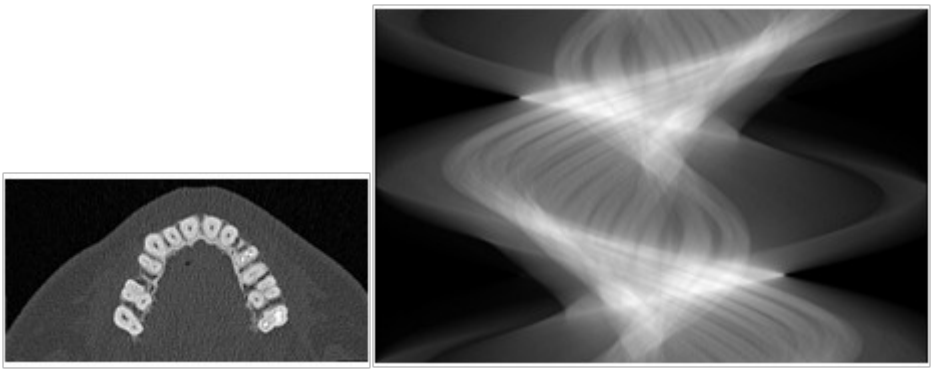

Fig. 5(A, B) A**:** B**:**

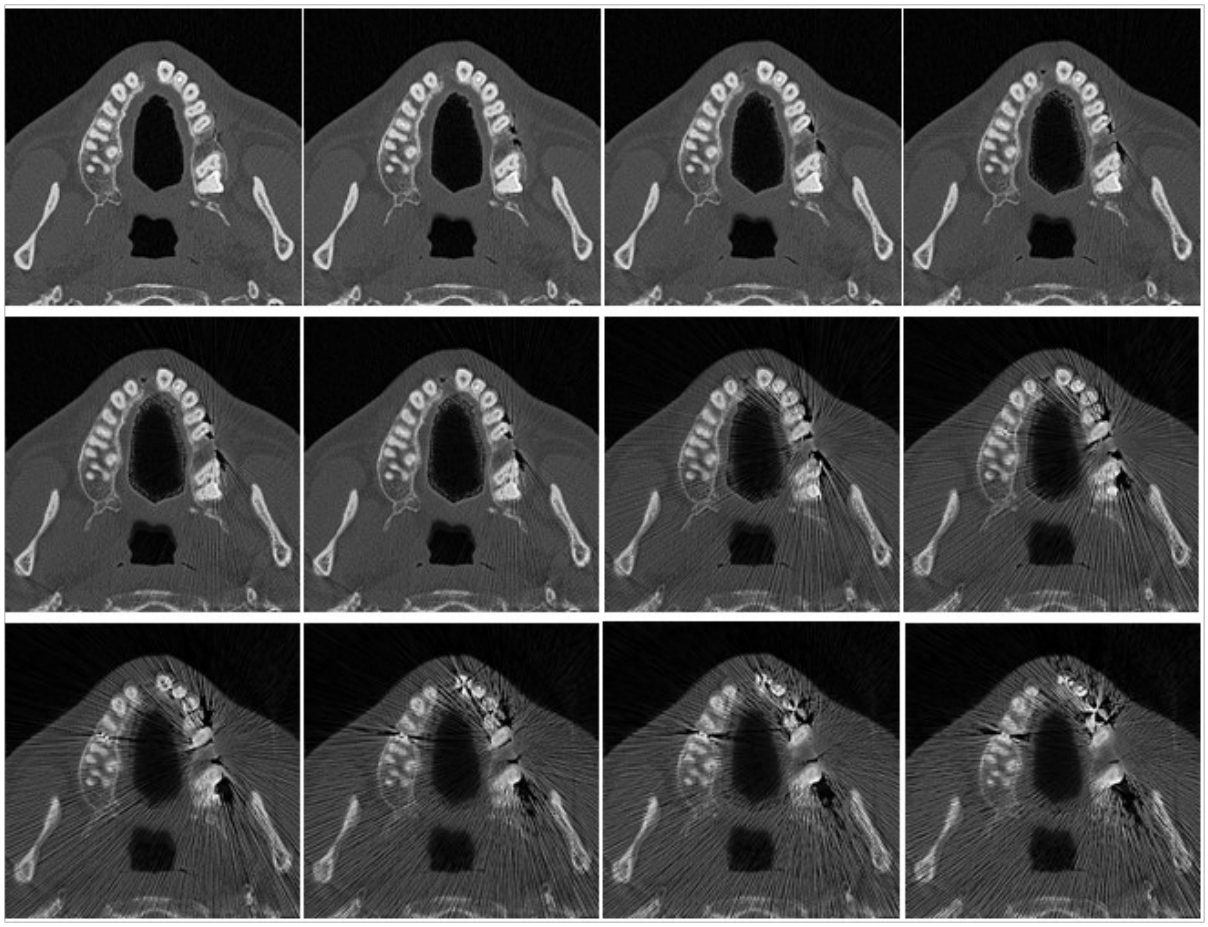

Fig.6

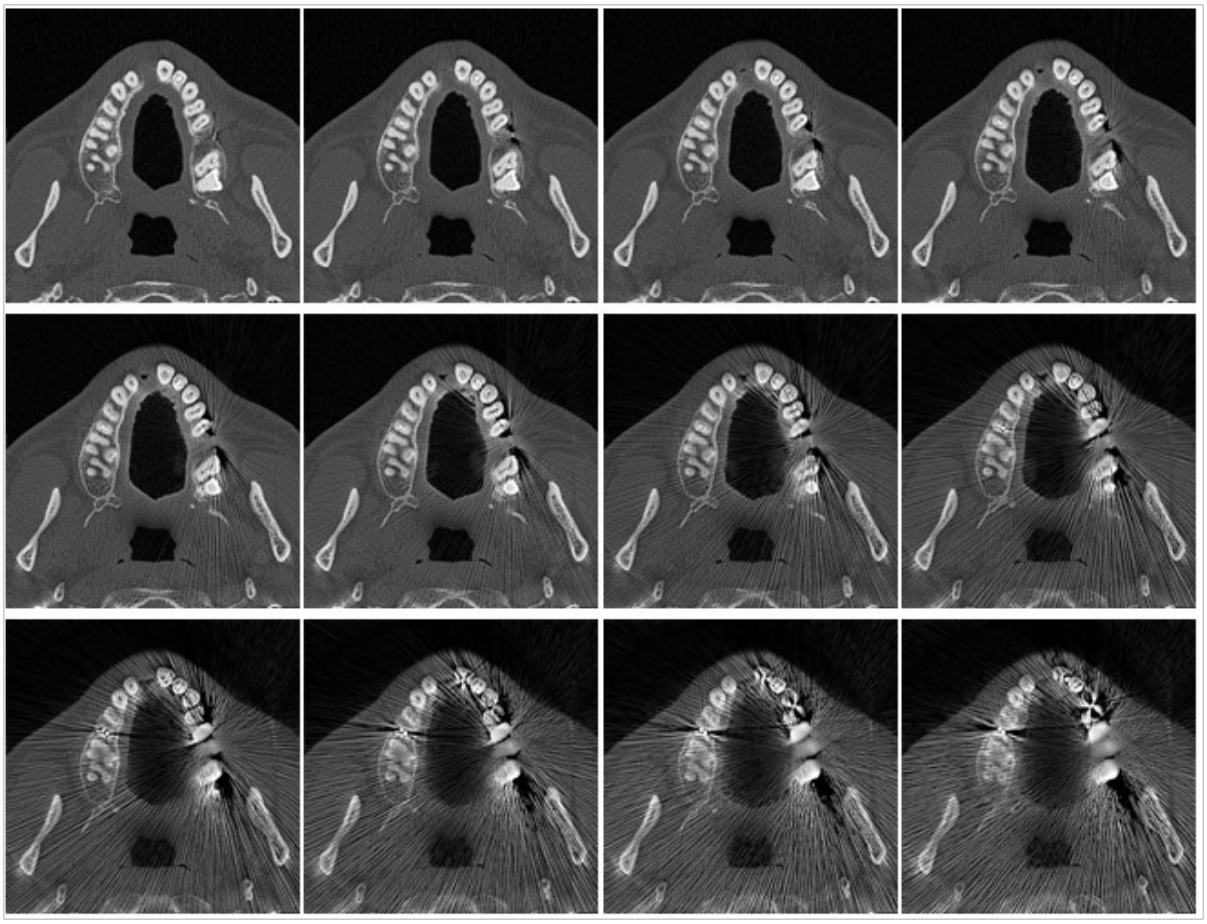

Fig.7

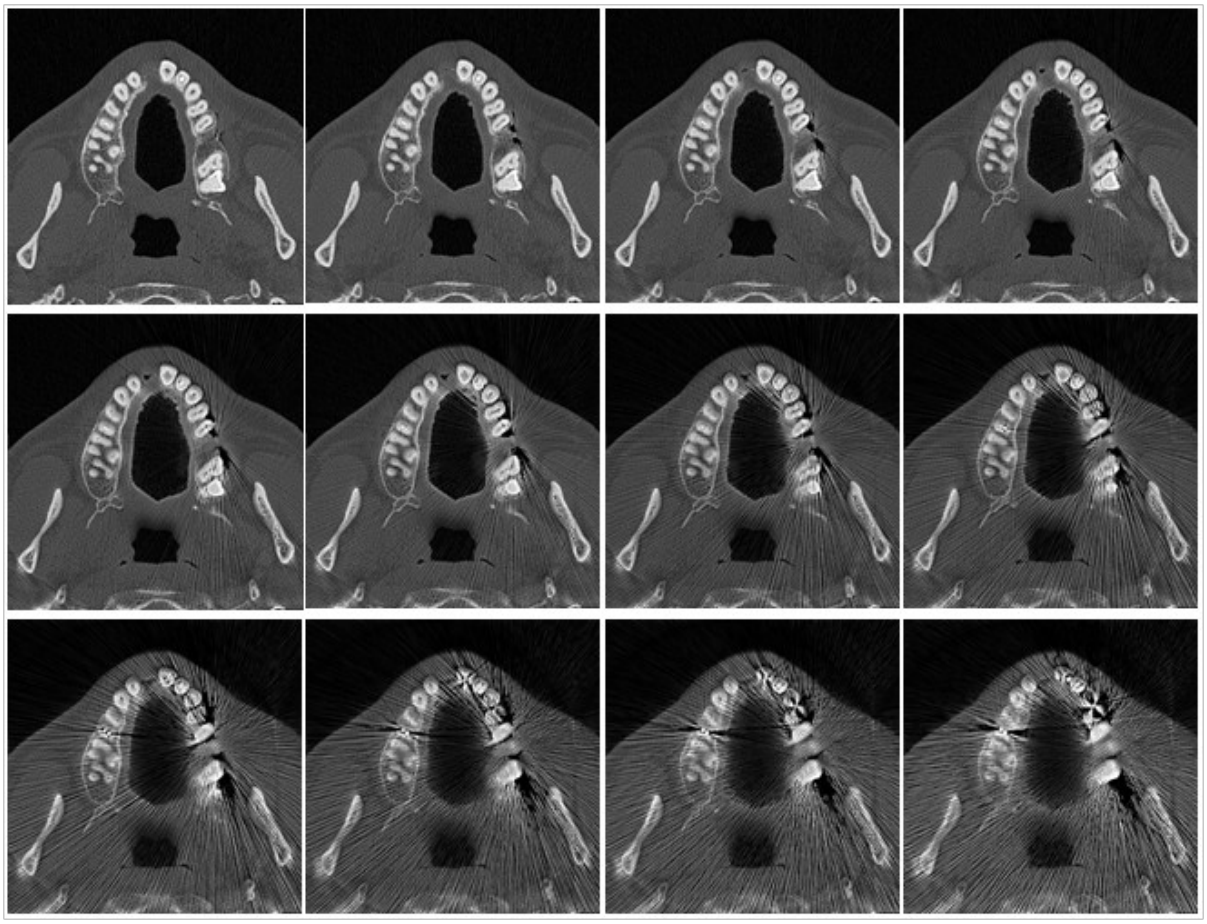

Fig.8

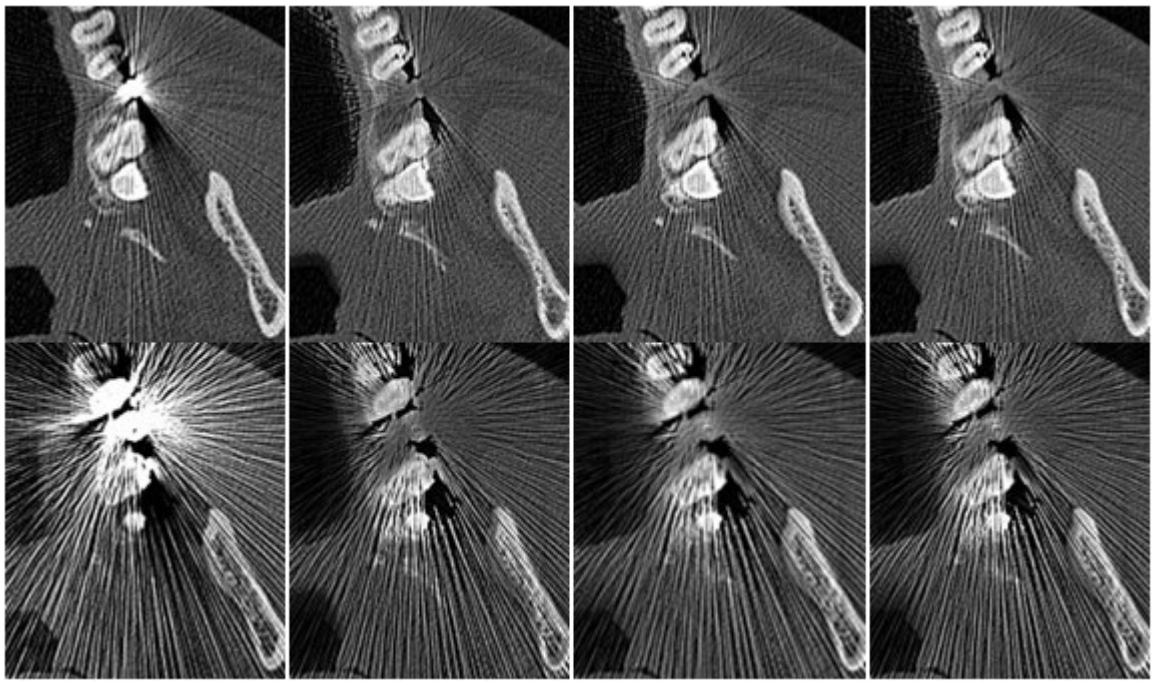

Fig.9

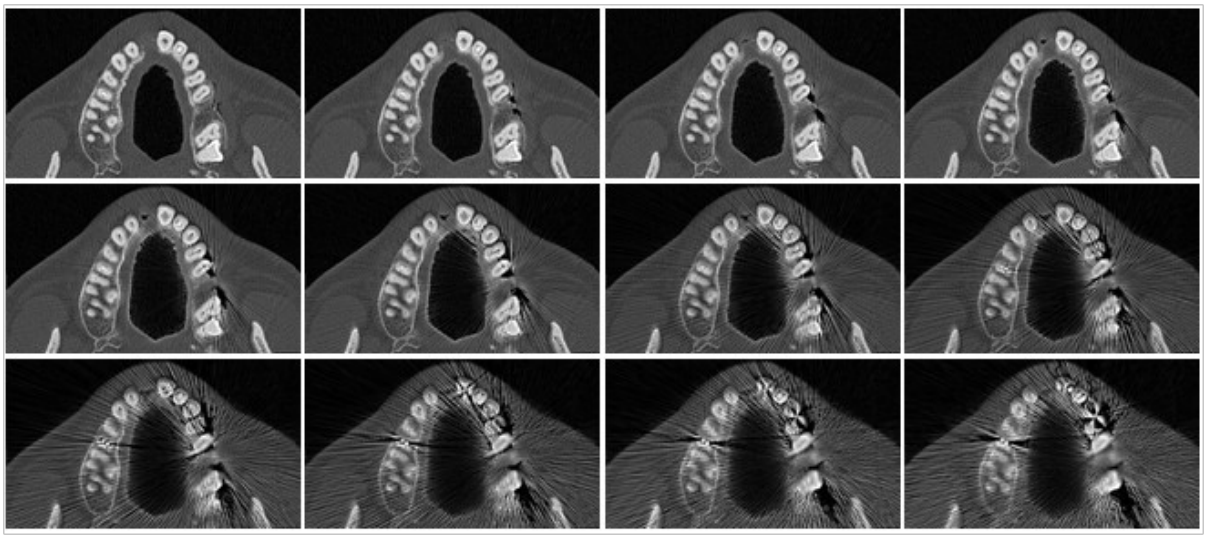

Fig.10

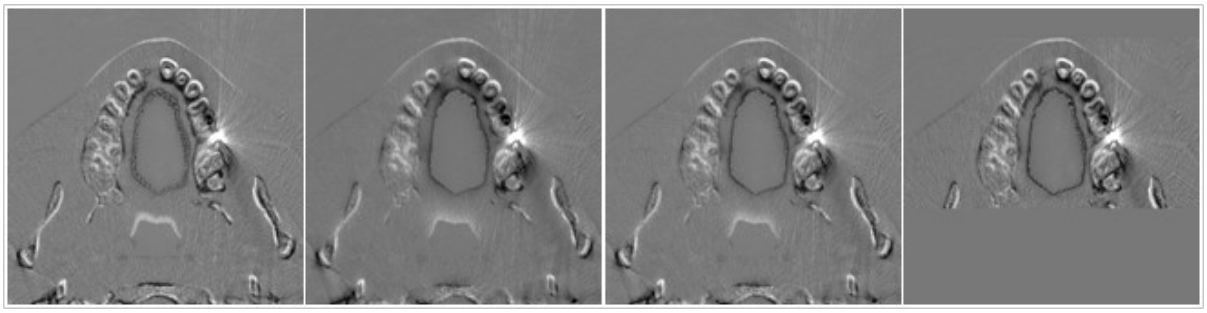

Fig.11

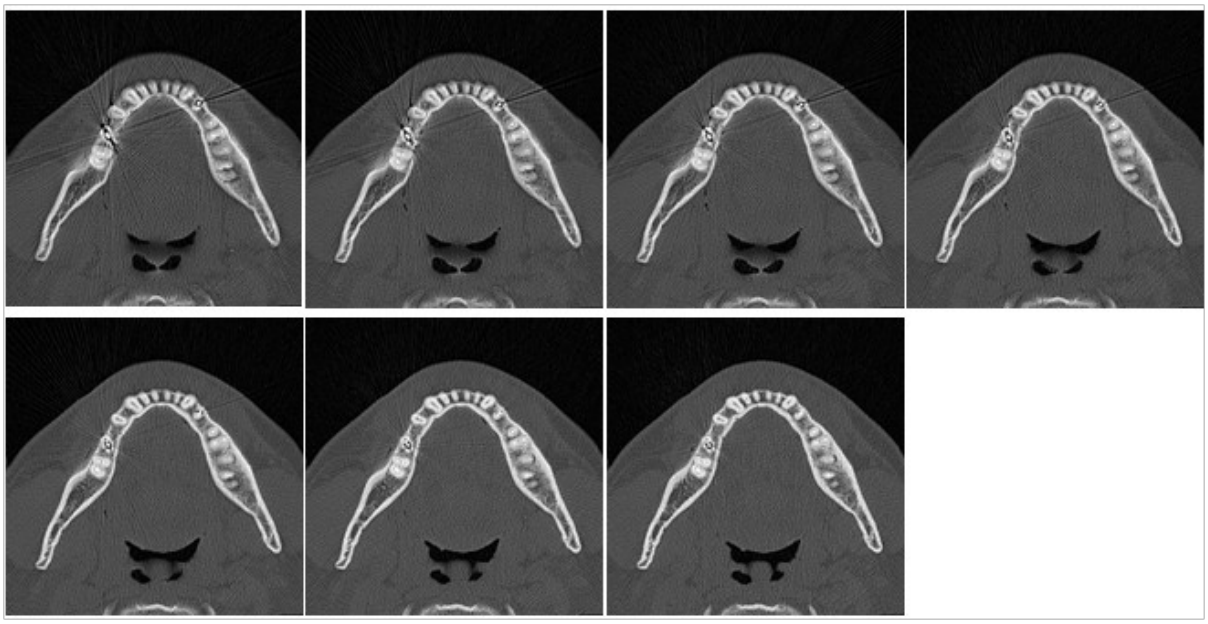

Fig.12

Table II. The duration time ratio of each method

ML-EM	Successive ML-EM	Successive OS-EM	Successive OS-EM with small ROI
1.0	1.0	0.227	0.124